# Ionization-Induced Instability in an Electron-Collecting Sheath

David L. Cook*
*Air Force Geophysics Laboratory, Hanscom Air Force Base, Massachusetts*
and
Ira Katz†
*S-Cubed, A Division of Maxwell Laboratories, La Jolla, California*

**An analytical and numerical investigation of the electron-collecting sheath about a positively biased probe in the ionosphere has been conducted to determine the effect of ionization within the sheath. This study is directed at the space charge-limited regime appropriate to objects having a characteristic size much larger than the ambient Debye length and a uniform surface potential much greater than the ambient plasma temperature. Computer calculations employing a fluid approximation were performed to study the dynamics of the secondary plasma produced within the sheath. Both the analytical and computational results indicate that, when the secondary ion production exceeds a critical level, the sheath edge propagates outward in an explosive fashion similar to the propagation of double layers. This critical level is shown to occur for sheath dimensions $D_s$ greater than about 1% of an ionization mean free path $\lambda$. This sheath size corresponds to the mean free path for ionization electrons reduced by the square root of the electron ion mass ratio $D_s > \alpha\lambda\sqrt{m_e/m_i}$, where $\alpha$ is a geometrical factor of order unity. At Shuttle altitudes and above, ionosphere probe interactions appear to be subcritical, but experiments with very high voltages, enhanced neutral background, or increased ionization by beam plasma discharge will trigger the instability.**

## Nomenclature

$a$ = acceleration
$D_{CL}$ = Child-Langmuir length
$D_d$ = double diode gap length
$D_s$ = sheath thickness
$e$ = electron charge
$F_{eo}$ = one-sided ambient electron thermal flux
$F_{es}$ = presheath enhanced ambient electron flux at sheath edge
$F_i$ = local or secondary ion flux
$F_n$ = one-sided ambient neutral flux
$H$ = potential well depth
$J$ = $eF$, current density with subscripting as $F$
$k$ = Boltzmann's constant
$m_e$ = electron mass
$m_i$ = ion mass (oxygen)
$m_n$ = neutral molecule mass (nitrogen)
$N_{ae}$ = ambient attracted electron density
$N_{ai}$ = ambient repelled ion density
$N_e$ = local or secondary electron density
$N_{es}$ = sheath edge ambient electron density
$N_i$ = local or secondary ion density
$N_n$ = ambient neutral density
$N_0$ = undisturbed ambient plasma density
$r$ = radial coordinate
$r_s$ = sheath radius
$r_i$ = ionization threshold radius
$r_w$ = potential well location
$r_0$ = probe radius
$S$ = local or secondary ion generation rate
$T$ = ambient plasma temperature, K
$u$ = velocity
$V$ = electrostatic potential
$V_p$ = probe surface potential
$V_s$ = sheath edge potential
$\alpha$ = anode factor
$\epsilon$ = electron kinetic energy
$\epsilon_0$ = permittivity of free space
$\lambda$ = mean free path for ionization of neutrals by electrons
$\lambda_D$ = Debye length
$\sigma$ = electron-neutral ionization cross section
$\bar{\sigma}$ = energy-averaged $\sigma(\epsilon)$
$\Omega$ = solid angle

(All units are in SI except as noted in text.)

Presented as Paper 85-7028 at the AIAA Shuttle Environment and Operations II Conference, Houston, TX, Nov. 13-15, 1985; received Feb. 27, 1987; revision received July 2, 1987. 

*Physicist, Space Physics Division. Member AIAA.
†Program Manager. Member AIAA.

## Introduction

IT has been suggested that some mechanism for ionizing the neutral gas near an ionospheric probe at a high positive potential is required to account for observed levels of electron current collection.[1] Early theoretical studies[2-4] that considered only the collection of ambient electrons tended to underestimate the return currents to an electron-emitting vehicle and overestimate the potential to which the vehicle charges. The predictions of these studies varied widely depending primarily upon the inclusion of magnetic field effects. Beard and Johnson[2] ignore the geomagnetic field; Parker and Murphy[3] include it, but mostly ignore space charge effects; and Linson[4] proposes "turbulence" to transport electrons across the magnetic field. The ionization of neutrals is considered by Zhulin et al.[5] and Galeev et al.,[6] but the only attempts at simultaneously including ionization and space charge (but not magnetic fields) are the related studies of Leadon et al.[7] and Lai et al.[8]

Figure 1 illustrates the sheath ionization problem in which electrons, attracted by the positive probe, fall through the sheath region and impact ionize neutral atoms with a cross section $\sigma$. The newly liberated secondary ions move out through the sheath and the secondary electrons are collected by the probe. A proper sheath model should include both ambient and secondary charge densities and be consistent with the solution of Poisson's equation. Lai et al.[8] does this

and predicts a nonmonotonic current-voltage characteristic that seems to be capable of explaining many observations, although the effect of the geomagnetic field is not included. Their method employs kinetic integral expressions for the secondary ion and electron space charge that are limited to monotonic sheath potential profiles.

Here, we present an analytical study of stability of electron-collecting sheaths to ionization of neutral atoms within the sheath. The analysis, based on the work of Langmuir,[9] makes use of many simplifying assumptions. Numerical simulations were performed to extend the results to conditions closer to those found in space experiments. The objectives of the simulations are twofold: 1) determine the relationship between the probe, plasma, and neutral background that could give rise, for typical geometries, to the ionization instability; and 2) model the early time evolution of the sheath when the parameters have exceeded the instability threshold. The emphasis is on the former.

Our computational model of sheath ionization employs a fluid approximation for the secondary ion space charge. This approach was chosen because it can easily accommodate nonmonotonic potentials, for its coding simplicity, and as a prototype for inclusion into the three-dimensional spacecraft charging simulation code POLAR,[10] where a requirement for computational efficiency precludes a more involved kinetic treatment. With this approach, we have been able to model sheath behavior as the secondary ion density in the (otherwise electron dominated) sheath reaches and exceeds a critical level. Specifically, the critical effect is that, with a sufficient internal secondary ion space charge, the sheath edge moves outward to include a more negative electron space charge; but, in doing so, the interior ion production is proportionally increased, leading to continued sheath expansion. This effect is closely related to the propagation of double layers[11] and will result in the elimination of the space charge sheath near the probe surface.

## Space Charge-Limited Sheath

This study of sheath ionization is conducted within the regime of space charge-limited current collection. This is equivalent to the short Debye length limit $\lambda_D \ll r_0$, where $\lambda_D$ is the Debye length and $r_0$ the probe radius. We also presume that the probe voltage is $V_p \gg kT/e$. Under these conditions, a plasma sheath may be described as composed of three regions: sheath, sheath edge, and presheath. The sheath is the region adjacent to the probe where only the attracted species is present from the ambient plasma and the potential decreases with radius $r$ faster than $r^{-2}$. This, combined with the assumption of high probe potential, produces a strong electric field that makes any orbital motion negligible and results in near-radial trajectories inside of some absorption radii. The sheath edge is the nominal absorption radius for the bulk of the attracted distribution and is generally a few $\lambda_D$ in thickness. The presheath is the quasineutral region that connects the sheath to the undisturbed plasma.[12] For equal plasma ion and electron temperatures, a spherical sheath edge locates at a potential of 0.49 $kT/e$, with the potential diminishing to zero at infinity through the presheath. In the following, we will not be concerned with the presheath.

## Diode Models

Under space charge-limited conditions, it is possible to approximate a plasma sheath as a space charge-limited diode,[13] where for electron collection the sheath edge is modeled as a virtual, electron-emitting cathode. The use of the term "space charge limited" for plasma probes actually comes from this analogy, where in the case of the diode it specifies a boundary condition of zero electric field on an emitting electrode due to the presence of an emitted space charge, which limits the emission current. We can obtain physical insight into the sheath ionization instability by pursuing the diode analogy.

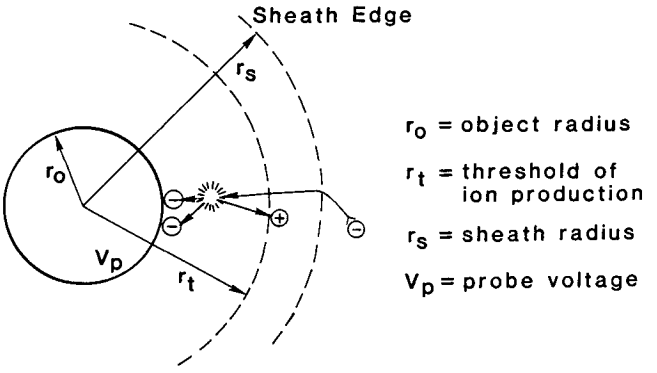


**Fig. 1 Ionization model configuration.**

Ionization occurring within the sheath, or diode, may be approximated by a double diode, a two-electrode device where charge carriers of opposite sign are emitted from opposing electrodes and transported across the intervening gap. In the analysis below, we shall employ such an approximation and, in following sections, validate it using computer simulations.

When there is no ionization or emission of ions by the anode (positive probe surface) and the geometry is planar, we have the usual Child-Langmuir[14,15] diode, where the electrode separation $D_{\mathrm{CL}}$, potential drop $V$, and current density $J$ are related by the expression

$$J_q = \frac{4\epsilon_0}{9}\left(\frac{2e}{m_q}\right)^{\frac{1}{2}} \frac{V^{\frac{3}{2}}}{D_{\mathrm{CL}}^2} \tag{1}$$

where $q = i$ or $e$ for electrons, respectively (all units are SI). If we use for $J_e$, the plasma thermal electron current density

$$J_e = N_e e(kT/2\pi m_e)^{\frac{1}{2}} \tag{2}$$

we may write

$$D_{\mathrm{CL}} = 1.26\lambda_D(eV/kT)^{\frac{3}{4}} \tag{3}$$

where $\lambda_D = \sqrt{\epsilon_0 kT/N_e e^2}$ is the plasma Debye length.

When a space charge limited ion current flows from the anode, we have Langmuir's double diode.[9] For the same electron current, the separation distance increase to

$$D_d = 1.36\ D_{\mathrm{CL}} \tag{4}$$

or if the separation is fixed, the currents will be 1.86 times the limit given by Eq. (1) with the same dependence on $D$ and $V$. It then follows from Eq. (1) that

$$J_e = \sqrt{m_i/m_e}\, J_i \tag{5}$$

In the generalization of the double diode to plasma double layers,[16] this relation is known as the "Langmuir condition" and is the basic stability requirement for a strong double layer. Figure 2 illustrates a double layer with anode and cathode locations indicated for comparison with a diode. If either flux should deviate, one sign of space charge in the layer will dominate and the layer will move upstream of the weaker flux so as to satisfy this condition in the moving frame of reference.

For the case of sheath ionization, ions need to be produced throughout the diode gap rather than at the anode. To our knowledge, the literature does not contain a complete solution for such a diode, although Langmuir[9] did analyze the problem for single ion release.

The literature for a diode formed of concentric spherical electrodes is sparse. We do have available the work of Lang-

muir and Blodgett,[17] who studied the single emitting electrode spherical diode. Their results are primarily tabular and are not reproduced here, but we note that Parker[18] provides a useful fit to those results. An interesting feature of their results is that, for a given potential drop and sphere radii, the limiting current (electrons) is higher for a central cathode than for a central anode. We account for this asymmetry in generalizing the Langmuir condition to spherical geometry with an anode factor $\alpha(r_1, r_2)$, thus,

$$J_i = \alpha\sqrt{m_e/m_i}\, J_e \tag{6}$$

The anode factor $\alpha$ must be determined numerically and has recently been reported by Wei and Wilbur.[19]

## Sheath Ionization Instability

The concept of the sheath ionization instability can be illustrated quite simply. Consider a positively biased spherical probe of radius $r_0$, sheath edge radius $r_s$, and a threshold radius $r_t$, where the electrons have attained sufficient energy $\epsilon$ to ionize neutrals with density $N_n$ and ionization cross section $\sigma(\epsilon)$. Inside $r_t$, the ion production rate will be

$$S(r) = \sigma[\epsilon(r)]\, N_n J_{ae}(r)/e \tag{7}$$

where $J_{ae}$ is the attracted ambient electron current density within the sheath. Assume that orbital motion within the sheath is negligible. Then, by continuity, we may relate $J_{ae}$ to $J_{es}$, the presheath enhanced[12] ambient electron flux absorbed at the sheath edge, as

$$J_{ae}(r) = J_{es}(r_s/r)^2 \tag{8}$$

An expression for the secondary ion current density out through the sheath edge can be obtained by integrating $S(r)$ over the volume of production and dividing by the sheath edge surface area,

$$J_i(r > r_t) = \bar{\sigma} N_n J_{es} \cdot (r_t - r_0) \tag{9}$$

where, for simplicity, we have replaced $\sigma[\epsilon(r)]$ with an average value $\bar{\sigma}$. By applying the Langmuir condition, we see that if

$$J_i > \alpha\sqrt{m_e/m_i}\, J_{es} \tag{10}$$

then the sheath will move outward, $\dot{r}_s > 0$, $\dot{r}_t > 0$, leading directly to an increase in $J_i$, which results in continued instability of the sheath. Of course, for low ionization, the sheath wants to move radially inward, but is stopped by the probe. From Eq. (9), we can see that Eq. (10) is equivalent to

$$\lambda < \sqrt{m_i/m_e}\,(D_s/\alpha) \tag{11}$$

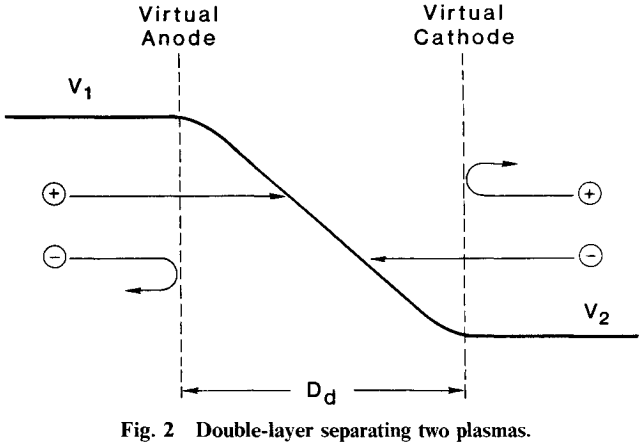


Fig. 2 Double-layer separating two plasmas.

where $\lambda = (\sigma N_n)^{-1}$ is the mean free path of electrons for ionization of neutrals and $D_s \simeq (r_t - r_0)$ is the sheath thickness. Linson[20] appears to have been the first to observe that the secondary or local ion space charge will be important for a mean free path much greater than the sheath thickness; however, he did not identify the attendant instability.

A careful estimate of the sheath expansion rate $\dot{r}_s$ is difficult to obtain, since the ion distribution function will depend on the specific potential distribution within the sheath and the energy dependence of the ionization cross section. However, we may typify the expansion by noting that it will be limited by the speed of the fastest ions, so

$$\dot{r}_s \simeq \sqrt{(2e\,\Delta V)/m_i} \simeq 10^4 \text{ m/s} \tag{12}$$

for oxygen atoms and a probe potential of 50 V.

There should certainly be mechanisms that will modify and limit the simple analysis present here. Some of these are:

1) A complex sheath potential profile may modify ion velocity distributions and cause some to impact the probe. Much of this effect will be included in the numerical model described in the next section.

2) Wave/particle interactions might preferentially retard electrons in the sheath and increase their space charge.

3) A magnetic field will modify electron trajectories in the sheath and possibly retain the ions in a halo where ambient heating could take place.[21]

4) Trapped orbits may be filled by secondary and scattered electrons. These will not be truly stable orbits unless there exists regions where the potential[22] falls off slower than $r^{-2}$, but our numerical studies indicate that such regions may appear as a sheath becomes unstable.

Neutral depletion is negligible, as can be seen from the ratio of outward ion flux $F_i$ to inward neutral flux $F_n$ at the sheath edge,

$$\frac{F_i}{F_n} = \sigma N_n D_s \frac{F_{es}\left(N_0, m_e^{-\frac{1}{2}}, T^{\frac{1}{2}}\right)}{F_n\left(N_n, m_n^{-\frac{1}{2}}, T^{\frac{1}{2}}\right)} = \bar{\sigma} N_0 D_s \sqrt{\frac{m_n}{m_e}} \tag{13}$$

where we have presumed identical temperatures and kinetic forms for the electron and neutral fluxes. Even for extreme choices of ambient electron density and sheath thickness, and $\bar{\sigma} = 2 \times 10^{-20}$ m$^2$, this ratio will remain exceedingly small.

Probe impedance will have a significant effect and is probably the major distinction between the numerical calculations presented here and those of Lai et al.[8] They modeled their probe as part of a constant-current circuit where the probe voltage fell as a result of the increased electron current produced by a sheath explosion. With a drop in probe voltage, the instability would be quenched by a reduction in the secondary ion flux, due to both a reduction in sheath thickness and electron energy. This effect will not be seen in our numerical model as our probe is held at a constant voltage and can support arbitrarily large currents.

## Numerical Model

A one-dimensional FORTRAN code, FLOMO, was written to model the sheath ionization problem. FLOMO is a self-consistant Poisson/space charge solver that iterates between Poisson and space charge solutions. Poisson's equation is solved directly by a simple tridiagonal method.[23] Space charge densities are obtained by a collection of models. Electrons are assumed to be quasistatic, with separate models for ambient and trapped secondary electrons. Ambient and secondary ions are followed separately with secondary ions modeled using time-dependent, single-fluid equations. The numerical grids have uniform $x$ (planar) and $r$ (spherical) spacings.

The repelled ambient ion density was modeled everywhere as $N_{ai} = N_0 \exp(-eV/kT)$. For the calculation of the attracted ambient electron density, a sharp-edge sheath ap-

proximation was used to separate different approximations that are matched at the sheath edge. For spherical geometry, the sheath edge conditions were taken from Parrot et al.,[12] who found that for $V_p \gg kT/e$ the sheath edge has potential $V_s = 0.49kT/e$, number density $N_{es} = 0.611N_0$, and flux density $F_{es} = 1.45F_{eo}$. Outside of the sheath, the attracted electron number density was taken from the following geometric fit to the results of Parrot et al.[12]:

$$N_{ae}(r) = N_0\left\{1 - 0.5\left[\frac{\Omega(r)}{2\pi}\right] + 0.11\left[\frac{\Omega(r)}{2\pi}\right]^2\right\} \quad (14)$$

where

$$\Omega(r) = 2\pi\left[1 - \sqrt{1 - (r_s/r)^2}\right] \quad (15)$$

represents the solid angle (shadow) subtended by the sheath. Inside the sheath edge, orbital motion is ignored and the attracted density is calculated by the usual continuity argument

$$N_{ae}(r) = (r_s/r)^2 F_{es}/u(r) \quad (16)$$

where velocity $u(r)$ is given by energy conservation

$$u(r) = \sqrt{u(r_s)^2 + 2e[V(r) - V_s]/m} \quad (17)$$

and where

$$u(r_s) = F_{es}/N_{es} \quad (18)$$

The secondary ion space charge is modeled as a fluid, using the continuity equation,

$$\frac{\partial N_i}{\partial t} + \frac{1}{r^2}\frac{\partial}{\partial r}r^2(N_i u) = S(r) \quad (19)$$

and the momentum equation

$$\frac{\partial(N_i u)}{\partial t} + \frac{1}{r^2}\frac{\partial}{\partial r}r^2(N_i uu) = N_i a(r) \quad (20)$$

where $a = qE/m$ is the single particle acceleration. The closure of Eqs. (19) and (20) is provided by Poisson's equation. These fluid equations are solved by finite differences using full upwind and forward time centering (explicit) on the convective terms.[23] This numerical scheme is outlined in the Appendix. This approach was chosen because of its robustness and its ability to handle nonmonotonic potential distributions, which is the particular advantage over an integral kinetic method. More rigorous methods such as a turning point formalism[22] or a fully differenced Vlasov approach[24] are beyond the scope of this work.

The secondary electron space charge is ignored unless local trapping occurs. We justify this by observing that in the absence of trapping, the secondary electron space charge is less than the ambient sheath electron space charge by more than a factor of $\sqrt{m_e/m_i}$.

After each Poisson solution, we inspect the potential distribution for the appearance of an electron trap, or well, and account for it as follows. Let us assume that a potential well of depth $H$ has appeared at $r_w$ and that in the well the electron distribution is Maxwellian for all trapped electron energies, zero for untrapped energies, and normalized to the central ion density $N_i(r_w)$, thus

$$N_e(r) = N_i(r_w)\cdot\left(\frac{m_e}{2\pi kT}\right)^{3/2} \cdot\exp\left[e\frac{V(r) - V(r_w)}{kT}\right]\cdot 4\pi\int_0^{u(H)} e^{-mu^2/2kT}u^2\,du$$
$$= N_i(r_w)\cdot\exp\left[e\frac{V(r) - V(r_w)}{kT}\right] \cdot\left[\operatorname{erf}\sqrt{\frac{eH}{kT}} - 2\sqrt{\frac{eH}{\pi kT}}\exp\left(-\frac{eH}{kT}\right)\right] \quad (21)$$

A secondary electron temperature of 1 eV was assumed in the calculations.

These various charge densities are summed and possibly adjusted according to a charge stabilization algorithm[10] that guarantees stability in the Poisson solution without iterate mixing.[25] Briefly, this algorithm derives from a physical plausibility argument which recognizes that, in the discretization of Poisson's equation, space charge features (such as the sheath edge) that are nonlinear with position and potential and numerical errors may both become artificially amplified when summed over discrete elements. The charge stabilization technique inspects for excessive total discrete charge and reduces it to a limit that is consistent with numerical stability.

## Results of the Numerical Calculations

We present the results from six calculations: a planar configuration with either no secondary ions, an anode ion source or volume ion production (ionization of neutrals), and a spherical configuration with the same secondary ion options. The planar calculation with anode ions and no local ions serves as a check on the accuracy of our model since those results may be compared with the analytic theory of Langmuir.[9] These calculations employed 100 grid points to span 30 m (planar) or 12 m (spherical). All six calculations employed the same ambient plasma parameters, which are summarized in Table 1 along with other model parameters. The steady-state results are presented in Table 2, where the sheath edge $D_S$ is found from the solution as the 0.5 $kT/e$ point. The results for

**Table 1 Model plasma parameters**

| | |
|---|---|
| $N_0 = 1.2\times10^9$ m$^{-3}$ | $\sqrt{m_i/m_e} = 242.2$ for oxygen |
| $kT = 0.04$ eV | $\lambda_D = 4.3\times10^{-2}$ m |
| $F_{e0} = 4.0\times10^{13}$ m$^{-2}$ s$^{-1}$ | $\sigma = 2\times10^{-20}$ m$^{-3}$ |
| $\epsilon = 10$ eV ionization threshold | |
| For $V_p = 50$ V | |
| $D_{CL} = 11.4$ m (Refs. 13 and 14) | |
| $D_d = 1.36\cdot D_{CL} = 15.5$ m (Ref. 15) | |
| For $R_0 = 2.0$ (spherical) | |
| $D_S = 4.0$ m (Refs. 10 and 16) | |

**Table 2 Numerical results[a]**

| Model | Sheath thickness, m: Model | Sheath thickness, m: Theory | Anode factor $\alpha$ | Critical neutral density $N_n$, m$^{-3}$ |
|---|---|---|---|---|
| Planar without local ions | 11.6 | 11.4 | — | |
| Planar with anode plasma | 15.9 | 15.5 | 1.05 | |
| Planar with ionization | 16.4 | — | 1.08 | $1.4\times10^{16}$ |
| Spherical without local ions | 4.4 | 4.0 | — | |
| Spherical with anode plasma | 6.5 | — | 2.1 | |
| Spherical with ionization | 5.7 | — | 2.3 | $7.0\times10^{16}$ |

[a] Sheath thickness, anode factors, and critical neutral density levels for the six models. Table 1 describes the plasma; the anode potential for $V_p$ was 50 V in all cases and the spherical probe radius was 2 m.

both the anode plasma and ionization models represent the saturation limit, i.e., if in either case the ion production is increased, the sheath edge begins to move outward. The sheath thickness given for the spherical models is $D_S = r_S - r_0$. The theoretical prediction for $D_S$ comes from Langmuir and Blodgett[16] using the presheath current enhancement of Parrot et al.[12]

The unstable motion of the sheath was investigated for the four cases that involved stability limits, but we present here only results for a marginally unstable spherical case. Figure 3 is a voltage radius profile for the 2 m radius spherical probe, with a neutral density of $5.0 \times 10^{16}$ $m^{-3}$. Notice that the sheath radius is ~ 6.4 m, which is essentially the result for no ionization. The charge densities are presented in Fig. 4.

In Fig. 5, the neutral density has been increased to $7.0 \times 10^{16}$ $m^{-3}$. The increase is modest, but the effect is dramatic resulting in an increase in sheath radius from 6.4 to 7.7 m, with a 45% increase in sheath area and ambient electron current. Figure 6 shows the charge density profiles where we see that electrons are still dominant inside the sheath.

If the neutral density is incremented to $8.0 \times 10^{16}$ $m^{-3}$, the unstable sheath expansion begins. Figure 7 is a voltage profile snapshot at 1.3 ms and Fig. 8 the charge profile. Notice how the ion density begins to dominate in some regions. As this occurs, the electric field that removes the ions is weakened, ion removal is reduced, and the density increases. The calculation was halted at 2.2 ms when the sheath hit the outer boundary at 14 m. This final set of profiles is shown in Figs. 9 and 10. It is noteworthy that all of our potential distributions are monotonic. This is due to the action of the secondary electron trapping model. Prior to its inclusion, unrealisticly large positive potential excursions were observed in the solutions, indicating that some trapping occurs.

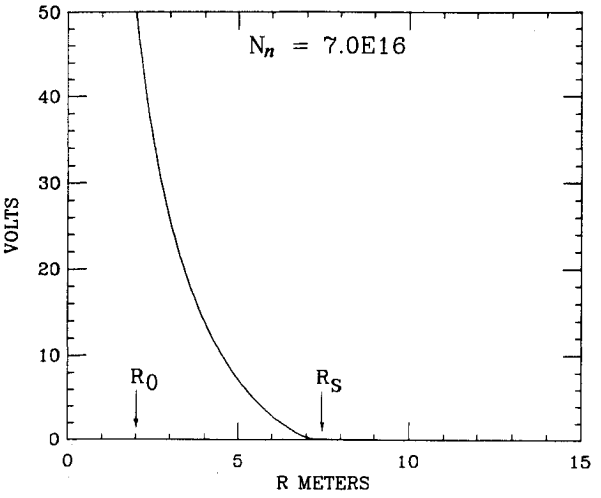


Fig. 5 Potential profile at maximum stable neutral density.

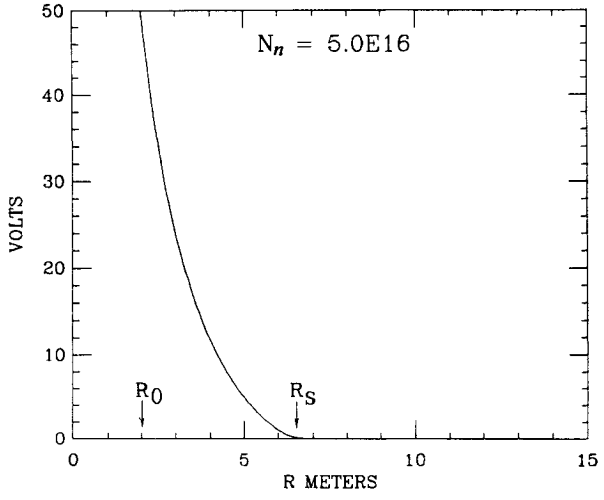


Fig. 3 Potential profile for low neutral density.

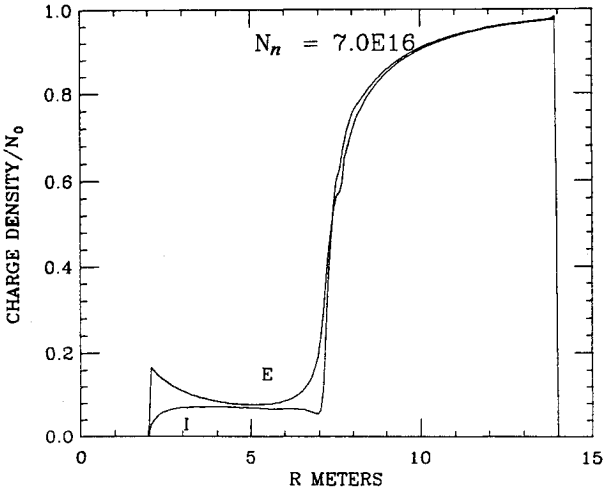


Fig. 6 Normalized charge density profiles corresponding to Fig. 5.

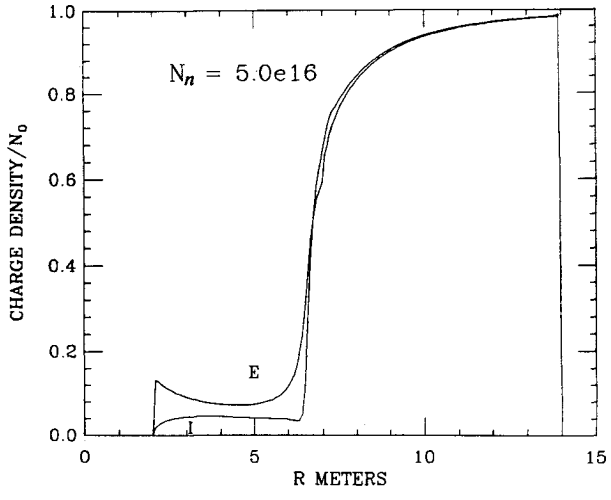


Fig. 4 Normalized charge density profiles corresponding to Fig. 3.

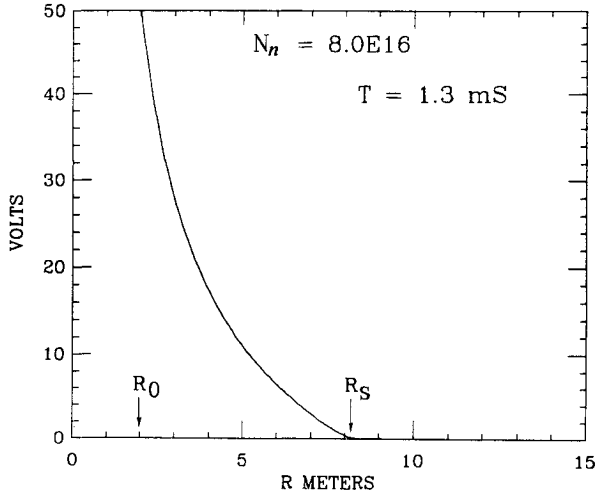


Fig. 7 Potential profile at $t = 1.3$ ms.

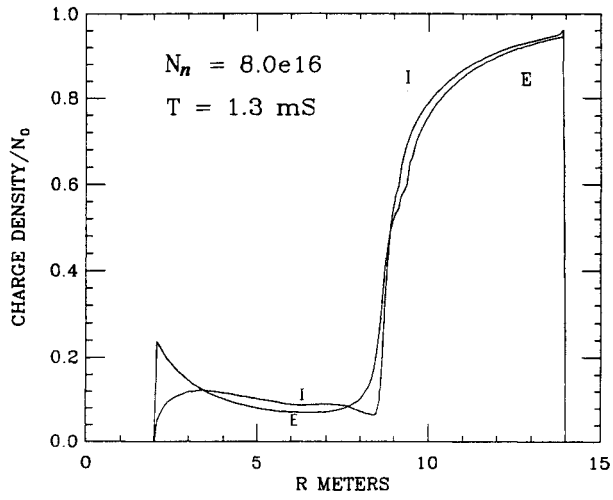


Fig. 8 Normalized charge density profiles corresponding to Fig. 7.

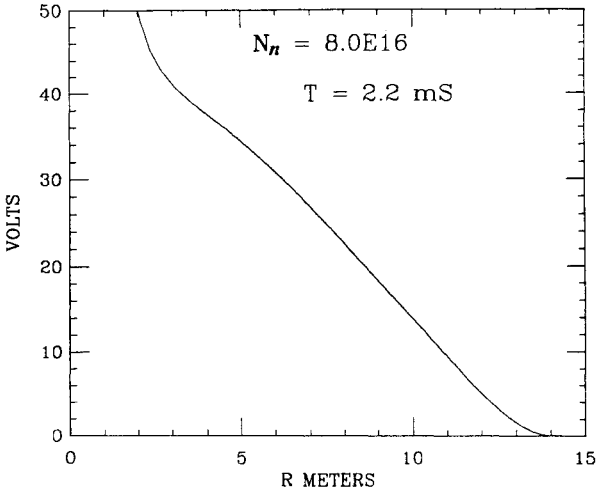


Fig. 9 Potential profile at 2.2 ms.

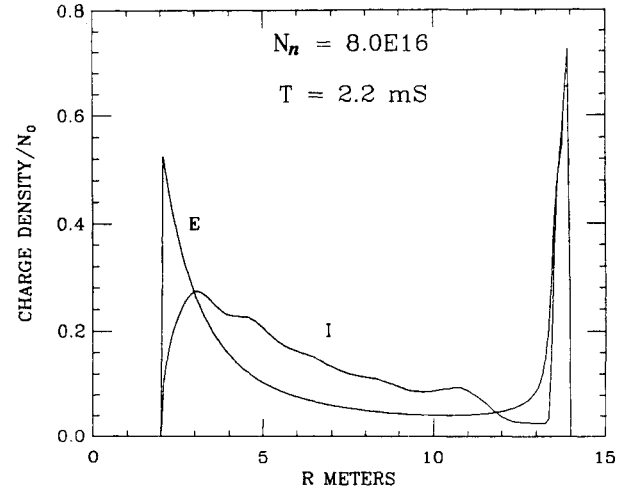


Fig. 10 Charge density profile corresponding to Fig. 9.

## Conclusions

The analogy between the volume ionization within a sheath and the Langmuir double-diode model appears well justified by the numerical results shown in Table 2. The ability of the sheath to expel ions appears relatively insensitive to where the ions are generated. This allows a very simple relation, Eq. (11), to determine whether sheath ionization will be important for a given experiment. The close agreement between our numerical calculations and Langmuir's double-diode theory[9] (Table 2) suggest that the numerical model is adequate. We also conclude that for a neutral density that is a factor of two or so below the critical level, ionization has little impact on electron collection or sheath structure.

The determination of the equivalent anode factor for the case of a spherical probe with sheath ionization is subject to numerical accuracy and this interesting number deserves more accurate evaluation. However, we may still obtain a conservative estimate of the critical neutral density from the planar results, since the anode factor is unity (the limit of $D_s \ll r_0$) and the planar sheath is thickest. Thus, from Eq. (11),

$$N_n = (\sigma D_d)^{-1}\sqrt{m_e/m_i} \tag{22}$$

or using Eqs. (3) and (4) and omitting constants of order unity,

$$N_n = (\sigma \cdot \lambda_D)^{-1}(kT/eV)^{\frac{3}{4}}\sqrt{m_e/m_i} \tag{23}$$

For a daytime shuttle environment, we might choose $kT/e = 0.1$ eV, $N_0 = 1 \times 10^{11}$ m$^{-3}$, $\lambda_D = 0.74$ cm, and $\sigma = 2 \times 10^{-20}$ m$^{-2}$. For these conditions, Eq. (11) predicts that a surface at a potential of 1 kV would develop an explosive sheath at $N_n \gtrsim 2 \times 10^{16}$ m$^{-3} \simeq 5 \times 10^{-7}$ Torr. In both this case and the previous model plasma, the critical neutral density is quite high compared to the natural background, but within the possible contamination range for the Shuttle and certainly important for sounding rockets.

## Appendix

The numerical fluid scheme of FLOMO is set into a staggered mesh where the secondary ion density $N_i$, secondary ion source rate $S$, and the electric field acceleration of secondary ions $a$ are defined on integral mesh nodes indexed as $j-1$, $j$, $j+1$, etc. (mass nodes). The ion velocity $u$ is defined at integrally spaced half-steps $j-\frac{1}{2}$, $j+\frac{1}{2}$, etc. (velocity nodes). Grid indices will appear as subscripts and the time index appears as a superscript to the right of a symbol. Upwind-differenced quantities are preceded by an asterisk. Volume-averaged quantities are covered by a bar and the sequence $+\ -$ indicates the sum of the plus and minus index quantity to be used in averaging, otherwise $\pm$ means the usual plus or minus.

Areas $A$ separating control volume elements (slabs or spherical shells) are defined at both integral and half-nodes and volume elements are calculated for each half-shell to facilitate volume averaging and the construction of both mass node and velocity node control volumes ($W_j$ and $W_{j+\frac{1}{2}}$, respectively) from the appropriate two half-volumes.

To simplify this outline, assume that the iteration sequence is underway, the grid indices are not on a boundary, and where for simplicity the usual $t$ and $t+1$ time indices are replaced by 0 and 1. The scheme then begins with calculating an upwind mass flux at velocity nodes,

$$*(Nu)^0_{j+\frac{1}{2}} = N^0_{j+\frac{1}{2}\pm\frac{1}{2}} \cdot u^0_{j+\frac{1}{2}} \tag{A1}$$

where the $\pm\frac{1}{2}$ indicates a choice of only the density "upwind" of $u_{j+\frac{1}{2}}$. Our differenced form for the continuity Eq. (19) is

$$\frac{N^1_j - N^0_j}{\Delta t} + \frac{A_{j+\frac{1}{2}}{}^*(Nu)^0_{j+\frac{1}{2}} - A_{j-\frac{1}{2}}{}^*(Nu)^0_{j-\frac{1}{2}}}{V_j} = S^0_j \tag{A2}$$

which may be algebraically solved for $N^1_j$.

Next, form the quantities,

$$(Nu)_j^0 = \overline{*(Nu)_{j+-\frac{1}{2}}^0} \tag{A3}$$

where a volume-weighted average is indicated by the notation (note that this term is not constructed upwind as the constituents are already upwind),

$$*u_j^0 = u_{j\pm\frac{1}{2}}^0 \tag{A4}$$

where the $\pm\frac{1}{2}$ indicates an upwind selection made according to the volume-averaged velocity $\overline{u_{j+-\frac{1}{2}}^0}$

$$N_{j+\frac{1}{2}}^1 = \overline{N_{j+\frac{1}{2}+-\frac{1}{2}}^1} \tag{A5}$$

With these definitions, we difference the momentum Eq. (20) as

$$\frac{\left(N_{j+\frac{1}{2}}^1 u_{j+\frac{1}{2}}^1\right) - \left(N_{j+\frac{1}{2}}^0 u_{j+\frac{1}{2}}^0\right)}{\Delta t} + \frac{\left(A_{j+1}(Nu)_{j+1}^0 * u_{j+1}^0\right) - \left(A_j (Nu)_j^0 * u_j^0\right)}{W_{j+\frac{1}{2}}} = a_{j+\frac{1}{2}}^0 N_{j+\frac{1}{2}}^0 \tag{A6}$$

which may be solved for $u_{j+\frac{1}{2}}^1$. The acceleration term is calculated as

$$a_{j+\frac{1}{2}}^0 = \frac{q\left(V_j^0 - V_{j+1}^0\right)}{m\left(r_{j+1} - r_j\right)} \tag{A7}$$

where $q$ and $m$ are the ion charge and mass.

The boundary condition on the probe surface ($j = \frac{1}{2}$) is

$$V_{\frac{1}{2}} = V_p, \qquad u_{\frac{1}{2}} = 0, \qquad N_0 = 0 \tag{A8}$$

On the outer boundary,

$$V = 0, \qquad u = 0, \qquad N = 0 \tag{A9}$$

where upwind differencing makes the choices for $u$ and $n$ inconsequential on the outflow boundary.

## Acknowledgment

The authors would like to acknowledge the late Milt Chapman for his aid in setting up the fluid numerics and Donald E. Parks for his consultation and advice throughout this project.

## References

[1]Winkler, J.R., "The Application of Artificial Electron Beams to Magnetospheric Research," *Review of Geophysics and Space Physics*, Vol. 18, 1980, p. 659.

[2]Beard, D.B. and Johnson, F.S., "Ionospheric Limitations on Attainable Satellite Potential," *Journal of Geophysical Research*, Vol. 66, 1961, p. 4113.

[3]Parker, L.W. and Murphy, B.L., "Potential Buildup on an Electron-Emitting Ionospheric Satellite," *Journal of Geophysical Research*, Vol. 72, No. 5, 1967, p. 1631.

[4]Linson, L.M., "Current-Voltage Characteristics of an Electron-Emitting Satellite in the Ionosphere," *Journal of Geophysical Research*, Vol. 74, No. 9, 1969, p. 2368.

[5]Zhulin, I.A., Kopaev, I.M., Koshelets, T.E., and Moskalenko, A.M., "On Rocket Charge Neutralization in Zarnitza Experiments," Institute Terrestrial Magnetism, Ionosphere, and Radio Wave Propagation, Academy of Science, USSR, Moscow, 1976.

[6]Galeev, A.A., Mishin, E.V., Sagdeev, R.Z., Shapiro, V.D., and Shevbenko, V.I., "Discharge in the Region Around a Rocket Following Injection of Electron Beams into the Ionosphere," *Doklady Academii Nauk SSSR*, No. 231, 1976, pp. 71-74 (in Russian).

[7]Leadon, R.E., Woods, A.J., Wenaas, E.P., and Klein, H.H., "Analytical Investigation of Emitting Probes in an Ionized Plasma," AFGL-TR-81-0138, 1980.

[8]Lai, S.T., Cohen, H.A., Bhavnani, K.H., and Tautz, M., "Sheath Ionization Model of Beam Emissions from Large Spacecraft," *Spacecraft Environmental Interactions Technology*—1983, NASA CP-2359, AFGL-TR-85-0018, 1985, pp. 253-262.

[9]Langmuir, I., "The Interaction of Electron and Positive Ion Space Charges in Cathode Sheaths," *Physical Review*, Vol. 33, 1929, p. 954.

[10]Cooke, D.L., Katz, I., Mandell, M.J., Lilley, J.R., Jr., and Rubin, A.J., "A Three-Dimensional Calculation of Shuttle Charging in Polar Orbit," *Spacecraft Environmental Interactions Technology*—1983, NASA CP-2359, AFGL-TR-85-0018, 1985, pp. 229-234.

[11]Carlqvist, P., "On the Formation of Double Layers in Plasmas," *Cosmic Electrodynamics*, Vol. 3, 1972, p. 377.

[12]Parrot, M.J.M., Storey, L.R.O., Parker, L.W., and Laframboise, J.G., "Theory of Cylindrical Langmuir Probes in the Limit of Vanishing Debye Number," *The Physics of Fluids*, Vol. 24, No. 12, 1982.

[13]Chen, F.F., "Electric Probes," *Plasma Diagnostic Techniques, Pure and Applied Physics*, Vol. 21, edited by R.H. Huddlestone and S.L. Leonard, Academic Press, New York, 1965, p. 232.

[14]Langmuir, I., "The Effect of Space Charge and Residual Gases on Thermionic Currents in High Vacuum," *Physical Review*, Vol. 2, 1913, p. 450.

[15]Child, C.D., "Discharge from Hot CaO," *Physical Review*, Vol. 32, 1911, p. 492.

[16]Block, L.P., "Potential Double Layers in the Ionosphere," *Cosmic Electrodynamics*, Vol. 3, 1972, p. 349.

[17]Langmuir, I. and Blodgett, K.B., "Currents Limited by Space Charge Between Concentric Spheres," *Physical Review*, Vol. 24, 1924, p. 49.

[18]Parker, L.W., "Plasmasheath-Photosheath Theory for Large High-Voltage Space Structures," *AIAA Progress in Astronautics and Aeronautics: Space Systems and Their Interactions with Earth's Space Environment*, Vol. 71, edited by H.B. Garrett and C.P. Pike, 1980, p. 477.

[19]Wei, R. and Wilbur, P.J., "Space-Charge-Limited Current Flow in a Spherical Double Sheath," *Journal of Applied Physics*, Vol. 60, Oct. 1986, pp. 2280-2284.

[20]Linson, L.M., "The Importance of Neutrals, Transient Effects, and the Earth's Magnetic Field on Sheath Structure," *Proceedings of Air Force Geophysics Laboratory Workshop on Natural Charging of Large Space Structures in Near Earth Polar Orbit*, AFGL-TR-83-0046, 1983.

[21]Cartwright, D.G., Monsoon, S.J., and Kellog, P.J., "Heating of the Ambient Ionosphere by an Artificially Injected Electron Beam," *Journal of Geophysical Research*, Vol. 83, 1978, p. 16.

[22]Laframboise, J.G., "Theory of Spherical and Cylindrical Langmuir Probes in a Collisionless, Maxwellian Plasma at Rest," UTIAS Rept. 100, 1966.

[23]Richtmyer, R.D. and Morton, K.W., *Difference Methods for Initial Value Problems*, Wiley-Interscience, New York, 1967.

[24]Rotenberg, M., "Transport Theory for Growing Cell Populations," *Journal of Theoretical Biology*, Vol. 103, 1983, pp. 181-191.

[25]Parker, L.W. and Sullivan, E.C., "Numerical Solution of the Poisson-Vlasov System for a Spherical Electrostatic Probe," Paper presented at Fall Meeting, Society of Industrial and Applied Mathematics, Philadelphia, 1970.